

J80-236

Flutter Analysis of Missile Control Surfaces Containing Structural Nonlinearities

Robert M. Laurenson* and Robert M. Trn†

McDonnell Douglas Astronautics Company, St. Louis, Mo.

00033
80001
80006

Missile control surfaces often contain nonlinearities which affect their performance characteristics and flutter boundaries. Analysis techniques accounting for these nonlinearities and an understanding of their potential influence on the flutter mechanism greatly increase the efficiency of the control surface design process. This paper presents such analysis procedures and discusses their application to the investigation of the dynamics of missile control surfaces containing structural freeplay-type nonlinearities. The problem discussed deals with a missile control surface exposed to subsonic flow. Nonlinearities are associated with freeplay in the root support stiffness. Definition of the loads acting on the control surface uses a simplified aerodynamic representation. The basic assumption of this approach is that the lift force is proportional to and in phase with the torsional, or pitch, motion. Both rigid and flexible control surface configurations have been examined with nonlinearities in either one or both of the root pitch or roll degrees-of-freedom.

Nomenclature

A	= amplitude of motion
A_r, A_{rd}, A_{er}, A_e	= rigid, rigid-elastic, and elastic aerodynamic loading matrices, see Eq. (2)
$I_\theta, I_\phi, I_{\theta\phi}$	= rigid control surface inertia properties, see Eq. (2)
K	= linear spring rate, see Fig. 2
\bar{K}	= effective stiffness
$L(t)$	= load developed in nonlinear spring
m_n	= generalized masses of control surface modes, see Eq. (2)
F_p	= inertia coupling matrix between rigid and elastic body motion, see Eq. (2)
q	= dynamic pressure
q_n	= generalized coordinates of control surface modes, see Eq. (2)
S	= deadspace, see Fig. 2
t	= time
δ	= describing function
θ	= root roll
ϕ	= root pitch
ω	= uncoupled frequency
$\bar{\omega}$	= effective frequency
Subscripts	
θ	= parameter associated with root roll
ϕ	= parameter associated with root pitch

Introduction

ALTHOUGH flutter is a dangerous phenomenon which can cause structural failure, it is possible to approach instability without destructive results. With the assumption of linear theory, there is a magnitude of dynamic pressure, or flight velocity, above which the system is unstable and the motion grows exponentially with time. However, as the

amplitude of oscillation begins to grow, the extent to which this increase continues depends upon the nature of the stiffness characteristics of the system. If the system is nonlinear, the system stiffness characteristics change with amplitude of motion and the oscillations may increase to some amplitude where the system experiences a stable limit cycle oscillation.

A missile control surface having a freeplay nonlinearity, or "slop," is an example of a system whose response characteristics are a function of the amplitude of oscillation. At a particular flight speed, the amplitude of oscillation, caused by external excitation, starts to build up. Due to the presence of a freeplay nonlinearity, in combination with increasing amplitude of oscillation, the effective stiffness of the system increases and the motion becomes stable at some limited amplitude. Thus, although the critical flutter speed of a linear configuration might be exceeded, destructive oscillations for a nonlinear system may not result from this tendency toward instability. The possibility of fatigue failure from large amplitude oscillations is, of course, not ruled out.

A flutter analysis technique accounting for these nonlinearities and an understanding of their potential influence on the flutter mechanism can increase the efficiency of the missile control surface design. By accounting for the presence of nonlinearities during the design process, additional confidence in defining a failure-free configuration can be realized.

In the past, limited analyses have been conducted to evaluate the influence of structural nonlinearities on missile control surface flutter. For example, the analyses of Refs. 1 and 2 were for a rigid control surface with a single nonlinearity. In these references, the nonlinear flutter problem was studied using basic linearization techniques and an analog computer. A review of some recent flutter analysis considerations including the influence of structural nonlinearities are discussed in Ref. 3. As mentioned in that report, there is a definite need for further development of analysis procedures to solve the nonlinear flutter problem with "several intensively interacting concentrated nonlinearities." The present study was undertaken to extend these results in order to: improve the techniques for including the influence of the nonlinearities in the dynamic analysis of control surfaces, remove the limitation of allowing only a single nonlinearity in the system, and develop techniques for flexible control surfaces having structural nonlinearities.

Specifically, the problem addressed during this study consisted of dealing with a missile control surface (Fig. 1)

Presented as Paper 79-0796 at the AIAA/ASME/ASCE/AHS 20th Structures, Structural Dynamics and Materials Conference, St. Louis, Mo., April 4-6, 1979; submitted June 18, 1980; revision received March 27, 1980. Copyright © American Institute of Aeronautics and Astronautics, Inc., 1979. All rights reserved.

Index categories: Aeroelasticity and Hydroelasticity; Structural Dynamics; Vibration.

*Senior Technical Specialist, Structural Dynamics Dept. Member AIAA.

†Engineer, Structural Dynamics Dept.

exposed to subsonic flow. A freeplay type of structural nonlinearity, illustrated in Fig. 2, was investigated during the study. This nonlinearity might represent a loose hinge or linkage of a control system or possible joint slippage. Structural nonlinearities were associated with the root rotational support springs K_θ and K_ϕ . Definition of the aerodynamic load acting on the control surface used the simplified representation defined in Refs. 4 and 5. The basic assumption of this approach is that the lift force is proportional to and in phase with surface pitch motion. The missile control surface flutter problem was represented by the following system of nonlinear equations

$$M\ddot{X} + K(X)X = qAX \quad (1)$$

Referring to Fig. 1, the detailed elements of Eq. (1) are given as

$$\begin{bmatrix} I_\phi & I_{\phi\theta} & PF \\ I_{\phi\theta} & I_\theta & 0 \\ PF^T & 0 & m_n \omega_n^2 \end{bmatrix} \begin{Bmatrix} \ddot{\theta} \\ \ddot{\phi} \\ \ddot{q}_n \end{Bmatrix} + \begin{bmatrix} K(\theta) & 0 & 0 \\ 0 & K(\phi) & 0 \\ 0 & 0 & m_n \omega_n^2 \end{bmatrix} \begin{Bmatrix} \theta \\ \phi \\ q_n \end{Bmatrix} = q \begin{bmatrix} A_r & A_{re} \\ A_{er} & A_e \end{bmatrix} \begin{Bmatrix} \theta \\ \phi \\ q_n \end{Bmatrix} \quad (2)$$

where the q_n 's are the generalized coordinates associated with the control surface modes. With no nonlinearities in the system, $K(\theta)$ and $K(\phi)$ are constants and not a function of system response.

During these investigations, the nonlinear flutter problem was analyzed through application of a linearization technique often referred to as the "describing function" approach. As discussed in Ref. 6, this technique is often used when dealing with nonlinearities in control systems. Application of the

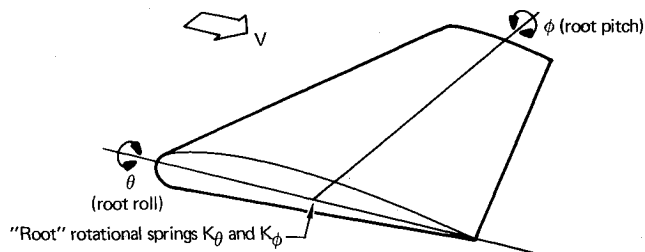


Fig. 1 Missile control surface.

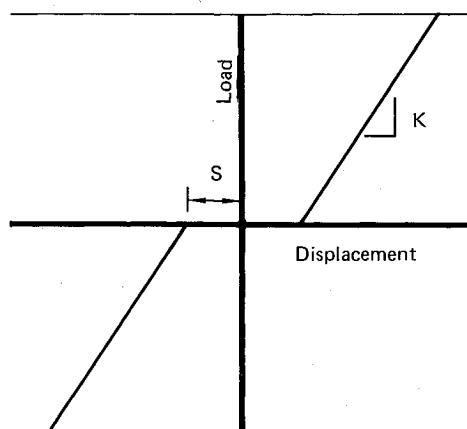


Fig. 2 Freeplay nonlinearity.

describing function approach for specific nonlinear control system elements is presented in Ref. 7.

The describing function technique is based upon a time-averaging approach for defining the input-output characteristics of a nonlinear system. It is assumed that for a sinusoidal input, the output is also sinusoidal with the same frequency as the input and that other harmonics can be neglected. Based upon these assumptions, the linearized quantities relating system output to input are expressed in terms of the fundamental component of the output's Fourier series representation. In the literature on mechanical vibrations, e.g., Ref. 8, this technique is often referred to as the method of harmonic balance.

Linearization Approach

As mentioned, a linearization procedure forms the basis of the developed flutter analysis procedures for missile control surfaces with structural nonlinearities. With this approach, the nonlinear equations of motion [Eq. (1)] are linearized for subsequent flutter analysis.

The basic approach for the method employed is to assume that the system displacement is sinusoidal and of the form

$$x(t) = A \sin t \quad (3)$$

For this displacement expression, the form of the load developed in the nonlinear spring is defined and this load relationship is then expanded in a Fourier series. The higher harmonics in the series expansion of the load time history are neglected. That is, for a sinusoidal input displacement, it is assumed that the output load is also sinusoidal with the same frequency. The ratio of the single-term Fourier series expansion of the developed load and the assumed displacement

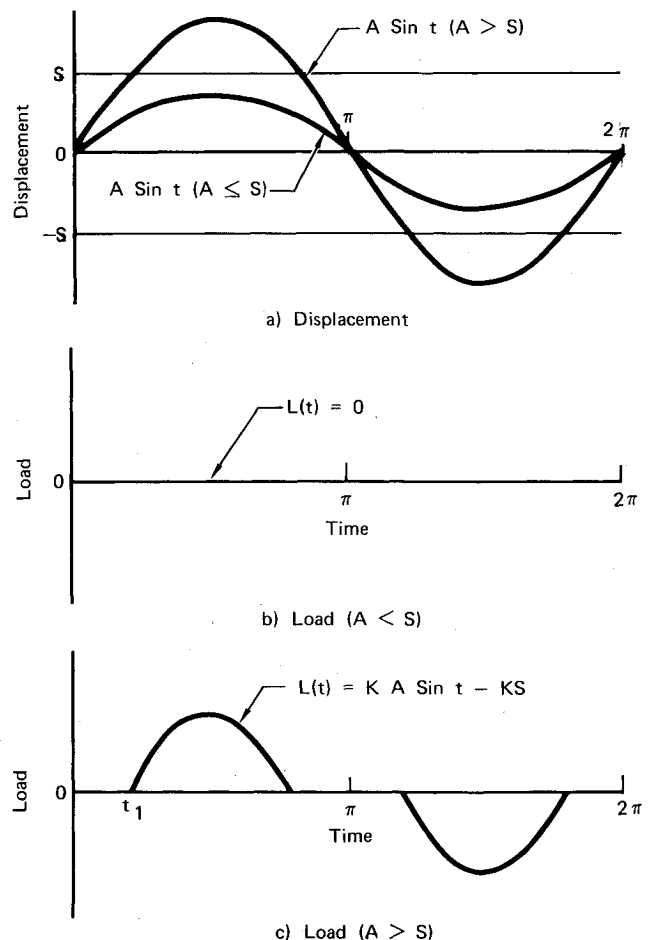


Fig. 3 Developed load for freeplay nonlinearity.

are then used to define an effective linear spring rate for the nonlinear element.

For a nonlinear spring with freeplay characteristics, as illustrated in Fig. 2, the waveform of the developed load may take one of the two shapes shown in Fig. 3. These waveforms are dependent upon the relationship between the magnitude of the freeplay and the amplitude of displacement [Eq. (3)]. For a displacement amplitude A less than the magnitude of the deadspace S , no load is developed (Fig. 3b). When A is greater than S , the developed load is as shown in Fig. 3c.

The effective stiffness \bar{K} of the nonlinear spring is defined as

$$\bar{K} = \delta K \quad (4)$$

In this expression, δ is the describing function which accounts for the presence of the freeplay nonlinearity. Using the describing function technique, we obtain a representation for the freeplay nonlinearity of the form

$$\delta = 0 \text{ for } A \leq S \quad (5)$$

and

$$\delta = (1/\pi) (\pi - 2t_1 - \sin 2t_1) \text{ for } A > S \quad (6)$$

where t_1 is given by

$$t_1 = \sin^{-1}(S/A) \quad (7)$$

Employing Eqs. (5) and (6), the relationship between the effective stiffness and the linear spring rate for a freeplay nonlinearity may be obtained. This relationship is shown in Fig. 4 as a function of the amplitude of motion to freeplay ratio. For amplitude ratios A/S less than one, the effective stiffness is zero. As the amplitude increases, the linear spring predominates and the magnitude of \bar{K} approaches that of K .

Flutter Analysis

The control surface flutter problem is represented by the system of nonlinear equations of motion given in Eq. (1). In the relationship of Eq. (1), $K(X)$ is the nonlinear system stiffness matrix. With no nonlinearities in the system, that is when $K(\theta)$ and $K(\phi)$ are constants and not a function of system response, standard solution techniques may be used to obtain flutter solutions of Eq. (1). At this point, the definition of the effective stiffness parameters given by Eq. (4) is employed. The nonlinear stiffness terms $K(\theta)$ and $K(\phi)$ in Eq. (1) are replaced with the corresponding effective parameters \bar{K}_θ and \bar{K}_ϕ associated with the assumed amplitudes of motion. In this manner the system equations of motion are linearized, and for specific values of \bar{K}_θ and \bar{K}_ϕ standard analysis techniques may be used to obtain flutter solutions.

The approach that has been used is to assume harmonic motion and conduct eigenvalue analyses for the resulting free vibration problem. For varying magnitudes of dynamic pressure, the form of the resulting complex eigenvalues is used to determine system stability, i.e., flutter. In addition to defining the flutter critical dynamic pressure, the flutter mode

shape is obtained during this eigenanalysis. From this mode shape, the relative root motions at flutter are defined.

Shown in Fig. 5 are linearized system results of dynamic pressure as a function of effective root roll uncoupled frequency $\bar{\omega}_\theta$. These results are for a flexible control surface whose characteristics are presented in the Appendix. The effective uncoupled frequency $\bar{\omega}_\theta$ is expressed as

$$\bar{\omega}_\theta = \sqrt{\delta_\theta} \omega_\theta \quad (8)$$

where ω_θ is the uncoupled frequency of the linear system. In this expression, δ_θ is the describing function for the nonlinearity in question and its magnitude depends upon the amplitude of motion in the root roll degree-of-freedom. A similar relationship holds for the root pitch parameter $\bar{\omega}_\phi$. Also shown in Fig. 5 are the relative magnitudes of motion in the nonlinear root springs defined by the eigenvectors of the linearized system.

The developed procedure modifies the flutter results obtained for the effective system (Fig. 5) to account for the presence of the nonlinearities. For the control surface of interest, a magnitude of root pitch freeplay is selected. For a freeplay nonlinearity in just the root roll degree-of-freedom, the initial step is to select magnitudes of root roll motion A_θ and effective root roll frequency $\bar{\omega}_\theta$. For the magnitude of A_θ , the describing function δ_θ is obtained from either Eq. (5) or (6). Using Eq. (8), the corresponding magnitude of root roll frequency ω_θ is determined. This is followed by obtaining the flutter dynamic pressure for the selected value of $\bar{\omega}_\theta$ from the effective system flutter results of Fig. 5. This procedure is then repeated for other values of $\bar{\omega}_\theta$ and A_θ and a relationship between dynamic pressure and the linear system root roll frequency ω_θ is obtained.

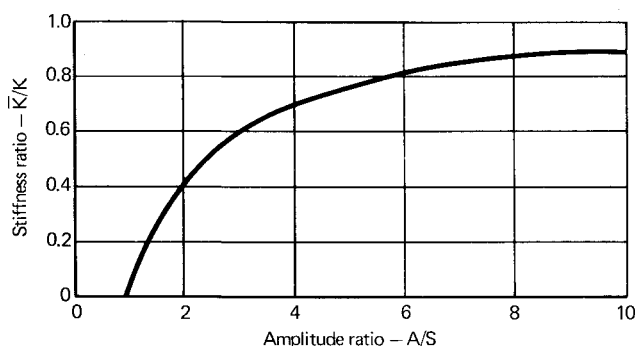


Fig. 4 Effective stiffness for freeplay nonlinearity.

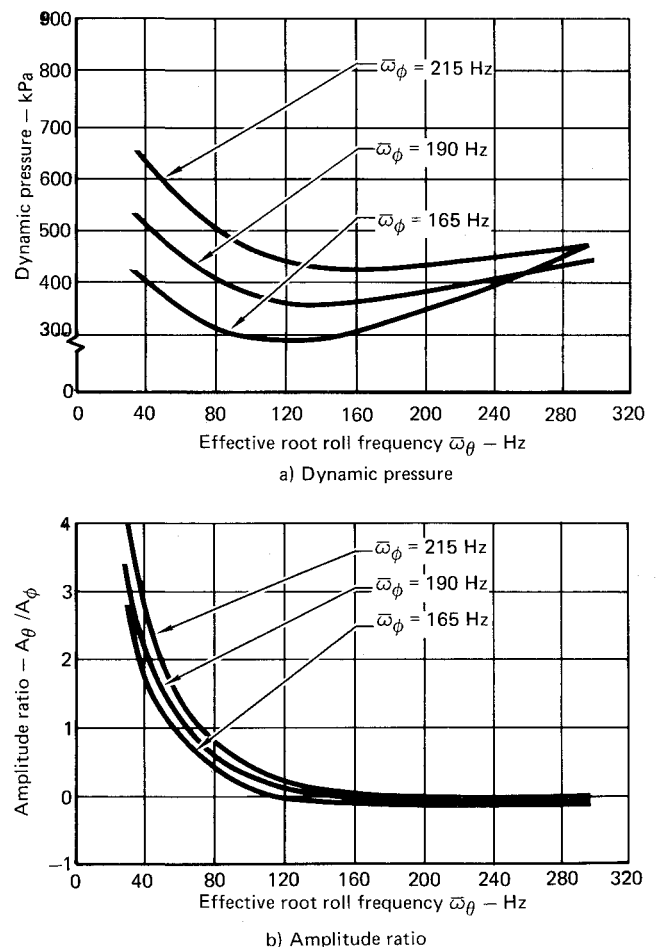


Fig. 5 Effective system flutter results.

For the case of a system with two nonlinearities, a value for the effective root roll frequency $\bar{\omega}_\theta$ is selected following the definition of the pitch freeplay. The flutter dynamic pressure and amplitude of motion ratio A_θ/A_ϕ corresponding to this value of $\bar{\omega}_\theta$ are obtained from the effective system flutter results of Fig. 5. Following evaluation of the relationship,

$$S_\theta/A_\theta = (S_\phi/A_\phi) (S_\theta/S_\phi) (A_\theta/A_\phi) \quad (9)$$

the magnitude of the describing function δ_θ is obtained from Eq. (5) or (6). Through application of Eq. (8), the corresponding linear system frequency ω_θ is then defined. This procedure is repeated for additional values of the parameter $\bar{\omega}_\theta$.

For either of these cases, one or two nonlinearities, the preceding steps lead to a definition of the flutter dynamic pressure as a function of the linear system frequency ω_θ . A family of these curves can be obtained which accounts for variations in the magnitude of root pitch freeplay.

Simulation Procedure

Ideally, the flutter predictions obtained with the described technique would be verified by comparing these predictions with experimental data obtained during a wind tunnel or flight test program. However, the expense of such a test program is high and thus "test" data were obtained through numerical simulations of the nonlinear flutter problem. With this approach, the nonlinear system equations of motion [Eq. (1)] were numerically integrated, yielding system time history response information. System stability characteristics were then obtained by evaluating the nature of this system response. It is emphasized that this process establishes only the validity (or shortcomings) of the describing function approach when compared to a more exact solution to the assumed mathematical representation of the nonlinear flutter problem. In the final evaluation, this approach does not replace the use of experimental or flight data.

The general approach in this verification process was to obtain numerical solutions to the nonlinear equations of motion for a control surface having particular root spring nonlinearities. These numerical solutions, which yield system time history response information, were used to evaluate system stability characteristics. System response was obtained for increasing values of dynamic pressure until the characteristics of the response became that of divergent oscillations. In this manner, the boundary between flutter and no flutter was evaluated for the nonlinear system.

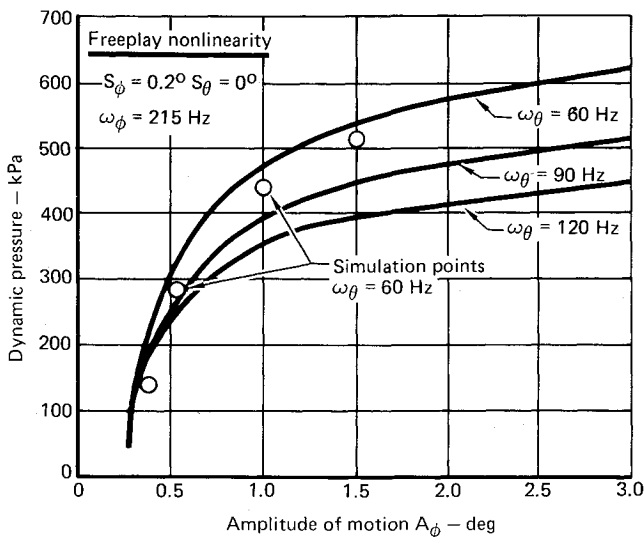


Fig. 6 Results for rigid control surface with root pitch freeplay nonlinearity.

Throughout the discussion of these simulation results, the characteristics of the system response will be expressed in terms of root sum squared (rss) amplitudes of motion. In many cases, the numerical solutions did not exhibit uniform amplitudes of motion, but rather demonstrated a beating type of phenomenon. This beating phenomenon is due to the nonlinear superposition of the root rotational modes and the flexible surface modes. To correlate these results with describing function predictions, an average amplitude of motion is employed. This rss amplitude is obtained by taking the square root of the sum of the squares of succeeding amplitude peaks over a large number of cycles of motion. Data obtained from simulations such as described above were compared with flutter predictions employing the describing function approach. In this manner the validity of these predictions was assessed.

Analysis Results

Results for a rigid control surface with a freeplay nonlinearity in the root pitch degree-of-freedom are shown in Fig. 6. These results are for a deadspace S_θ of 0.2 deg and

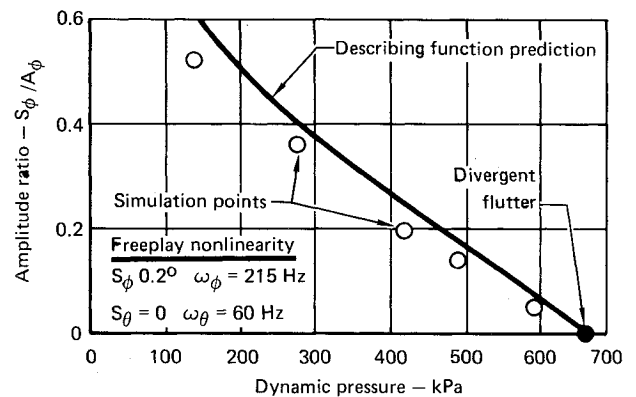


Fig. 7 Root pitch motion for root pitch nonlinearity.

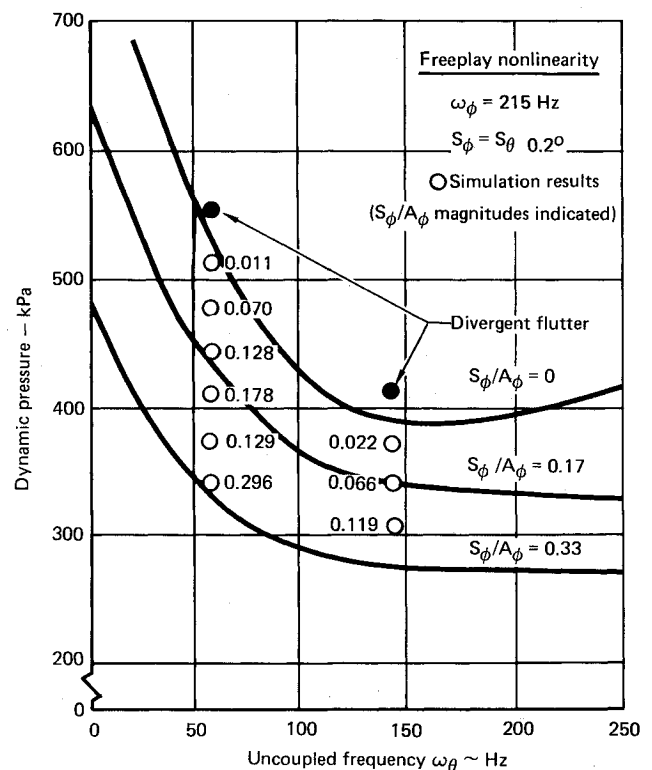


Fig. 8 Results for flexible control surface with two root freeplay nonlinearities.

various uncoupled root roll frequencies ω_θ . Comparisons between simulation results and describing function predictions for this case are also shown in Fig. 6. Note that for the simulation results the assumed root stiffness values result in uncoupled frequencies ω_θ of 60 Hz and ω_ϕ of 215 Hz.

A characteristic response for the nonlinear system appeared throughout this study. For increasing magnitudes of dynamic pressure, the system response tends to become divergent in nature. However, this has the effect of working the nonlinear root spring to a greater extent. Thus the oscillation builds up to some amplitude and again becomes stable with the system experiencing limit cycle oscillation. This trend of stable limit cycle response with increasing dynamic pressure is illustrated in Fig. 7. In Fig. 7 simulation data points, which correspond to the data of Fig. 6, are related to describing function predicted amplitudes of motion. Increasing amplitude of motion corresponds to a decreasing S/A amplitude ratio. As indicated in Fig. 7, the amplitude of motion increases with increasing dynamic pressure until the point of divergent flutter is reached.

The effective system flutter results for a flexible control surface shown in Fig. 5 are converted to a definition of the flutter dynamic pressure accounting for the presence of two root freeplay nonlinearities as illustrated in Fig. 8. These results are presented as a function of the linear system uncoupled root roll frequency ω_θ . The family of curves shown in

this figure account for variations in the amplitude of motion ratio S_ϕ/A_ϕ .

For the case of two system nonlinearities, the dynamic pressure vs effective root roll frequency curve corresponding to the linear system uncoupled root pitch frequency in Fig. 8, S_ϕ/A_ϕ equal zero, represents a divergent flutter boundary. The remaining curves are indicative of the stable limit cycle amplitudes of oscillation for dynamic pressures below the critical flutter value.

Also shown in Fig. 8 are the simulation results for the flexible control surface with nonlinearities in both root degrees-of-freedom. These simulation results are for a system with equal deadspace in the two root degrees-of-freedom which were assumed to be 0.2 deg. In addition, the assumed root stiffnesses result in an uncoupled frequency ω_θ of 215 Hz and uncoupled frequencies ω_ϕ of either 60 or 140 Hz.

As in the case with a single nonlinearity, the system experiences stable limit cycle response with increasing dynamic pressure. Shown in Fig. 8 are simulation data points related to the resulting S_ϕ/A_ϕ ratios of this motion. Above some critical dynamic pressure, the limit cycle motion no longer holds and we have the classic divergent flutter motion. These results are further illustrated in Fig. 9 where a comparison of simulation and describing function predictions are presented as a function of dynamic pressure.

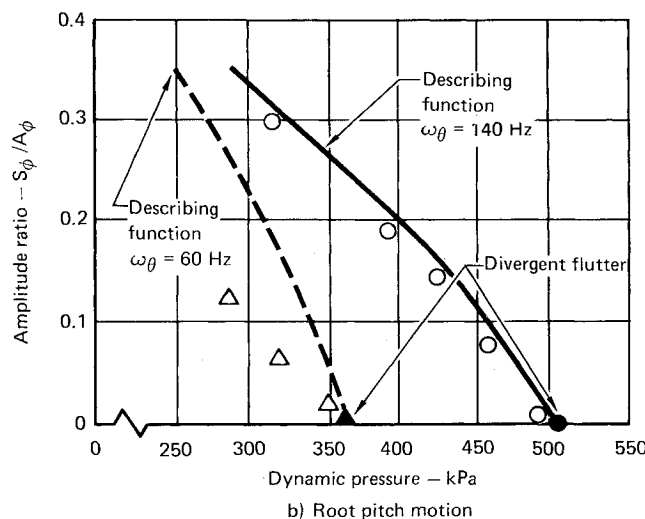
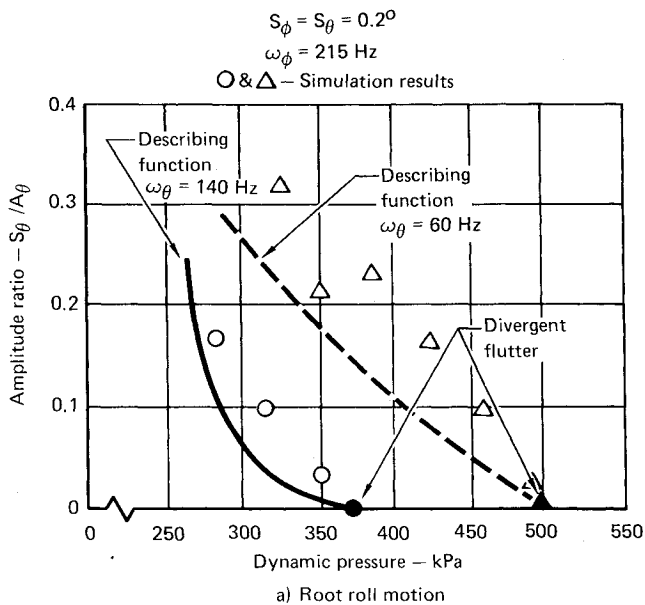


Fig. 9 Root motions for two root nonlinearities.

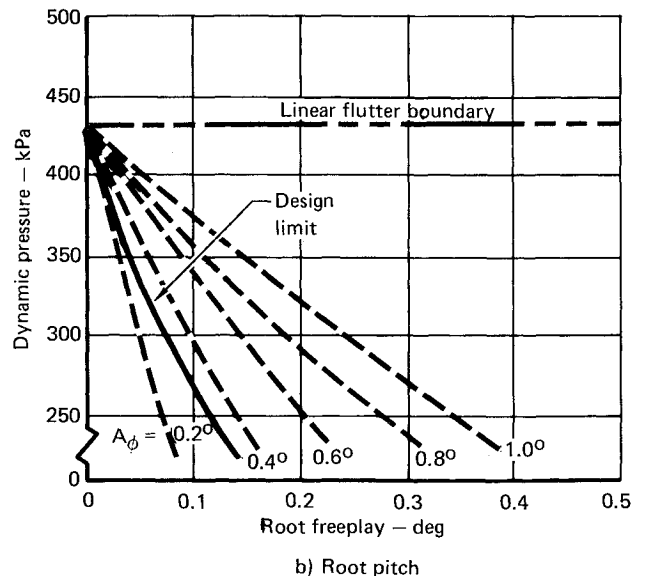
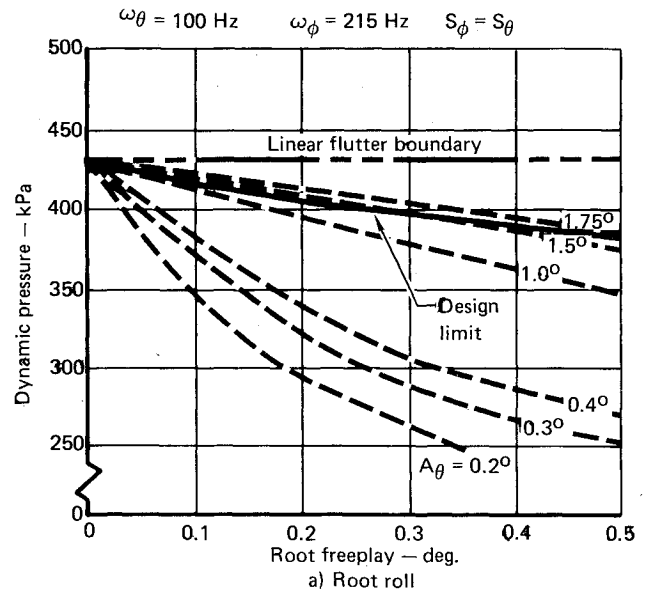


Fig. 10 Design limit for two root nonlinearities.

Conclusions

An understanding of the control surface flutter mechanism as influenced by nonlinearities in the root support stiffness has been developed. The interrelationship between the magnitude of the nonlinearities, flight conditions, and the nature of the resulting control surface response has been investigated. Since the flutter speed is a function of the natural frequency of the system, the change in natural frequency attendant on the increased amplitude of oscillation alters the critical flutter speed. The presence of a freeplay nonlinearity tends to cause the effective system stiffness to be less than that of the linear system. This relationship, or stiffness ratio, between effective and actual system stiffnesses is dependent upon the amplitude of motion being experienced by the control surface system.

The developed analysis procedure to account for system nonlinearities employs a describing function technique. The describing function approach has the advantage that it is much more efficient than the numerical simulation approach. Also of advantage is the fact that its use is based upon the modification of linear system flutter results which are obtained during the normal missile control surface design process. The describing function approach was applied to flutter results obtained using simplified aerodynamics. It is reasonable to expect that the approach can be extended to use in conjunction with unsteady aerodynamic procedures.

The basic characteristic of the response for the control surface system with freeplay nonlinearities was such that for increasing magnitudes of dynamic pressure, the system response tends to become divergent in nature. However, this has the effect of working the structural nonlinearity to a greater extent. Thus the oscillation builds up to some amplitude and again becomes stable. This trend of stable response continues with increasing dynamic pressure. Above some critical dynamic pressure, the stable motion no longer exists and we have the classic divergent flutter motion. The amplitude predictions below divergent flutter are useful from a design point of view. Prediction of these steady oscillations for flight conditions below flutter may be related to load and fatigue considerations in the control surface and related subsystem design.

An example of the results which may be obtained when using the developed procedures to predict operating limits based on loading conditions is presented in Fig. 10. These figures are for a control surface having equal freeplay nonlinearities in both root degrees-of-freedom. Presented in Fig. 10 is the family of curves, defined by dotted lines, depicting dynamic pressure vs magnitude of root freeplay for various magnitudes of limit cycle oscillation. Assuming that

the moments in the root roll and root pitch springs must be less than 57 and 147 N·m, respectively, the maximum deflection in each root spring may be determined. Here it has been assumed that these are limits on the oscillating loads which are in addition to trim and maneuver loads. Thus, the maximum limit cycle oscillation in each spring is this deflection plus the magnitude of freeplay. Cross plotting these limiting magnitudes of oscillation (solid lines in Fig. 10) defines the indicated design limit. This design limit gives the dynamic pressure at which the limits on the load increment will be exceeded for a particular freeplay nonlinearity.

For the particular case presented here, it can be seen that the system is very sensitive to the amount of the freeplay in the pitch degree-of-freedom. As shown in Fig. 10, an increase of 0.05 deg in pitch freeplay results in a decrease of 70 kPa in dynamic pressure for maximum allowable load. This indicates that the freeplay tolerance for the pitch degree-of-freedom is more critical than the roll degree-of-freedom for success of the design. In addition, as illustrated in Fig. 10, the limit on dynamic pressure from a loads point of view may be quite a bit less than the predicted linear flutter boundary.

The situation of a control surface having a freeplay plus preload nonlinearity has also been investigated.⁹ The effective stiffness of a freeplay plus preload nonlinearity is a double-valued function. A particular magnitude of effective stiffness is associated with two different amplitudes of motion. When the system tends to become unstable for an effective stiffness associated with an amplitude of motion below the deadspace, the motion "jumps" across the deadspace. At some higher amplitude the system will again experience stable limit cycle oscillations. As discussed in Ref. 9, the describing function approach may be used to characterize the response trends of a control surface containing freeplay plus preload nonlinearities.

Appendix

Properties of the control surface configuration used throughout the study are shown in Fig. A1. The nonlinearities that were investigated are associated with the root support stiffness.

Referring to Eq. (2), the inertia properties of the control surface are as follows:

$$I_{\theta} = 0.0188 \text{ kg} \cdot \text{m}^2 \quad PF_{\theta 1} = -0.0321 \text{ kg} \cdot \text{m}$$

$$I_{\phi} = 0.0080 \text{ kg} \cdot \text{m}^2 \quad PF_{\phi 2} = -0.0045 \text{ kg} \cdot \text{m}$$

$$I_{\theta\phi} = 0.0065 \text{ kg} \cdot \text{m}^2 \quad PF_{\phi 1} = -0.0143 \text{ kg} \cdot \text{m}$$

$$m_1 = 0.0738 \text{ kg} \quad PF_{\phi 2} = 0.0095 \text{ kg} \cdot \text{m}$$

$$m_2 = 0.0752 \text{ kg}$$

The first two rows and columns of the inertia matrix are associated with rigid root roll and pitch motions while the last two diagonal elements are the generalized masses of the control surface modes. The off-diagonal terms, the PF quantities, represent the inertia coupling between rigid and flexible motions. The first two control surface cantilever modes are a 163 Hz bending mode and a 419 Hz twist mode. These modal data were used when investigating a flexible control surface configuration.

Acknowledgment

This work was supported by the Department of the Navy, Naval Air Systems Command, under Contract N00019-76-C-0524. The program monitor for this work was Allan Somoroff. Details of this contracted work are presented in Ref. 9.

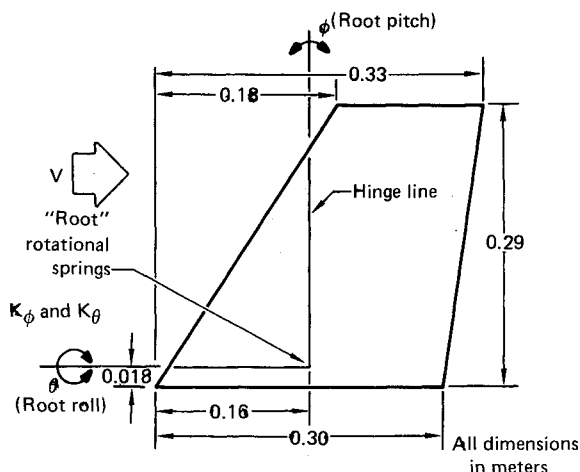


Fig. A1 Control surface geometry (all dimensions in metrics).

References

- ¹Woolston, D. S., Runyan, H. L., and Andrews, R. E., "An Investigation of Effects of Certain Types of Structural Nonlinearities on Wing and Control Surface Flutter," *Journal of the Aeronautical Sciences*, Vol. 24, Jan. 1957, pp. 57-63.
- ²Shen, S. F., "An Approximate Analysis of Nonlinear Flutter Problems," *Journal of the Aerospace Sciences*, Vol. 26, Jan. 1959, pp. 25-31, 45.
- ³Breitback, E., "Effects of Structural Non-Linearities on Aircraft Vibration and Flutter," AGARD-R-665, Jan. 1978.
- ⁴Zimmerman, N. H., "Elementary Static Aerodynamics Add Significance and Scope in Flutter Analyses," AIAA Symposium on Structural Dynamics of High Speed Flight, Los Angeles, Calif., April 24-26, 1961.
- ⁵Pines, S., "An Elementary Explanation of the Flutter Mechanism," *Proceedings of the National Specialists Meeting on Dynamics and Aeroelasticity*, Fort Worth, Texas, Nov. 6-7, 1958.
- ⁶Hsu, J. C. and Meyer, A. V., *Modern Control Principles and Application*, McGraw-Hill Book Co., Inc., New York, 1968, Chap. 6.
- ⁷Gelb, A. and Vander Velder, W. E., "On Limit Cycling Control Systems," *IEEE Transactions on Automatic Control*, April 1963, pp. 142-157.
- ⁸Magnus, K., *Vibrations*, Blackie & Sons Ltd., London, 1965, pp. 108-112.
- ⁹Laurenson, R. M. and Trn, R. M., "Flutter of Control Surfaces with Structural Nonlinearities," McDonnell Douglas Astronautics Co., St. Louis, Mo., MDC E1734, Aug. 1977.

From the AIAA Progress in Astronautics and Aeronautics Series..

EXPERIMENTAL DIAGNOSTICS IN COMBUSTION OF SOLIDS—v. 63

Edited by Thomas L. Boggs, Naval Weapons Center, and Ben T. Zinn, Georgia Institute of Technology

The present volume was prepared as a sequel to Volume 53, *Experimental Diagnostics in Gas Phase Combustion Systems*, published in 1977. Its objective is similar to that of the gas phase combustion volume, namely, to assemble in one place a set of advanced expository treatments of the newest diagnostic methods that have emerged in recent years in experimental combustion research in heterogenous systems and to analyze both the potentials and the shortcomings in ways that would suggest directions for future development. The emphasis in the first volume was on homogenous gas phase systems, usually the subject of idealized laboratory researches; the emphasis in the present volume is on heterogenous two- or more-phase systems typical of those encountered in practical combustors.

As remarked in the 1977 volume, the particular diagnostic methods selected for presentation were largely undeveloped a decade ago. However, these more powerful methods now make possible a deeper and much more detailed understanding of the complex processes in combustion than we had thought feasible at that time.

Like the previous one, this volume was planned as a means to disseminate the techniques hitherto known only to specialists to the much broader community of research scientists and development engineers in the combustion field. We believe that the articles and the selected references to the current literature contained in the articles will prove useful and stimulating.

339 pp., 6 × 9 illus., including one four-color plate, \$20.00 Mem., \$35.00 List

TO ORDER WRITE: Publications Dept., AIAA, 1290 Avenue of the Americas, New York, N.Y. 10019